

NUMERICAL ANALYSIS OF STRESS DISTRIBUTION IN TOTAL HIP REPLACEMENT IMPLANT NUMERIČKA ANALIZA RASPODELE NAPONA U TOTALNOJ ZAMENI ZGLOBA KUKA

Originalni naučni rad / Original scientific paper

UDK /UDC: 617.581-77:612.766

612.766:519.6

Rad primljen / Paper received: 2.10.2017

Adresa autora / Author's address:

¹⁾ University of Belgrade, Innovation Centre of the Faculty of Mechanical Engineering, Serbia

²⁾ University of Belgrade, Faculty of Mechanical Engineering, email: asedmak@mas.bg.ac.rs

Keywords

- total hip replacement implant
- Co-Cr alloy
- stress distribution
- finite element method
- fatigue crack

Abstract

Total hip replacement implants represent permanent implants and require large bone and cartilage removal during implantation. Revision would affect joint capability to sustain load, which makes this procedure irreversible. During exploitation, i.e. everyday activities, implants are subjected to dynamic loading. Thereby, these structures are prone to failure by fatigue. Highest stress states on total hip replacement implants are present in the neck area of the implant, which is a position of crack initiation. Under loading the implant neck exhibits tension and compression zones. Crack initiation in the neck side under tension would lead to crack opening and certain fracture. Implants are examined by experimental and numerical methods. The most common numerical method is finite element method (FEM) used to simulate different loading conditions. In this paper numerical analysis of stress distribution in the neck area is performed on a specific implant. Four numerical models are created in order to show how certain design solutions influence the stress distribution in the neck area.

INTRODUCTION

Total hip replacement implants are used to restore joint function in a diseased hip, and require complete removal of hip joint. Implants have limited lifespan and of greatest concern is the problem of implant failure. Failure can be caused by implant loosening, dislocation, wear of material. Due to dynamic loading, wherewith implants are subjected throughout everyday use, fatigue represents a most probable mechanism of structural failure, /1, 2/.

Total hip replacement implants can be classified into two types according to design. Non-modular design is a one-part implant, and modular consists of stem, head, cup and metal back, /3/. The hip joint is formed of acetabulum, is a concave surface of the pelvis and femur head, /4/. The acetabulum is superseded by a cup and metal back. Stem is a bearing element of the implant, inserted into the medullary cavity of femur. Stem neck taper holds the ball head, /1, 3/. Contact of ball head and cup allows motion of the hip joint. The subject of this paper is numerical analysis of stress distribution on modular stem 'Zimmer VerSys[®] CRC', Fig. 1.

Ključne reči

- implant za totalnu zamenu zgloba kuka
- Co-Cr legura
- raspodela napona
- metoda konačnih elemenata
- zamorna prslina

Izvod

Implanti za totalnu zamenu zgloba kuka su stalne proteze, čijom ugradnjom se uklanja velika količina kosti i hrskavice. Ova procedura je nepovratna, jer bi revizija smanjila mogućnost zgloba da prenese opterećenje. U eksploataciji, odnosno, tokom svakodnevnih aktivnosti, implantati su pod dejstvom dinamičkih opterećenja. Time su ove strukture sklone lomu nastalom usled zamora. Najviša naponska stanja kod implanata za totalnu zamenu zgloba kuka su prisutna u zoni vrata, gde je moguć nastanak prslina. Pod opterećenjem u vratu proteze se javljaju zone istezanja i sabijanja. Stvaranje prslina na delu vrata koji je opterećen na zatezanje doveo bi do otvaranja prslina i sigurnog loma. Implantati se ispituju eksperimentalnim i numeričkim metodama. Najčešće korišćena numerička metoda je metoda konačnih elemenata, kojom se simulira mehaničko ponašanje. U ovom radu je izvršena numerička analiza raspodele napona u zoni vrata određenog implanta kuka. Napravljena su četiri numerička modela kako bi se pokazao uticaj određenih rešenja u dizajnu na raspodelu napona u zoni vrata.



Figure 1. Total hip replacement implant 'Zimmer VerSys[®] CRC'.

Total hip replacement implants are exposed to high influence of dynamic loading, which appears during everyday activities, /5, 6/. Fatigue occurs in places with highest stress states. Defects in the structure, such as inclusions and micro cracks, influence the stress state but are not taken into account in numerical analysis. Locations with highest stress concentration are only considered for predicting fatigue crack initiation. Most common place where failure appears on a total hip replacement implant is the neck area, on sharp edges where stress states are the highest. The loaded neck area of the implant contains zones of tension and compression. An unfavourable location of crack initiation is the tension zone, where the normal stresses tend to open the crack until the cross-section of the material is insufficient to sustain the load. Implants are designed to reduce stress concentration on the tension side of the neck and to create maximal stress concentration on the compression side of the neck, where the eventual crack would be pressed by material preventing its further propagation.

The largest measured force exerted on a hip joint is 8.7 times body weight, generated during stumbling, /4/. In this study, stress distribution on the neck area of implant is obtained for a static load equal to the maximal load applied on the implant. The subject of this paper is the influence of implant geometry on the stress distribution in the neck area, thereby analysis is performed only for the modular stem. Contact bone-implant is compensated with adequate boundary conditions, /7, 8/. Material properties of specified implant design are obtained from literature. The finite element method is a modern numerical method for predicting mechanical behaviour. It includes a development of the numerical model and discretization with finite elements. Complexity of the model and the required accuracy determine the shape and size of finite elements.

On a selected modular stem (Fig. 1) there are certain openings and one hole (Fig. 2), which are assumed to have influence on the stress distribution in the neck area. Four numerical models with a different set of openings and hole are obtained in order to show their individual influence. Based on stress the distribution in the critical area for crack initiation, the aim of this paper is to show how these solutions influence structural life of the specific implant.

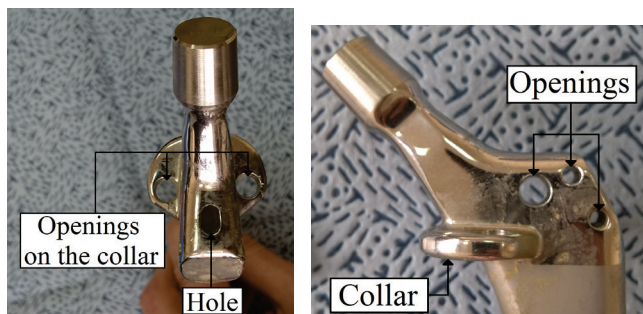


Figure 2. Total hip replacement implant 'Zimmer VerSys® CRC', (left) top view; (right) side view.

It is worth mentioning that the human body is a highly corrosive environment, which greatly affects initiation and growth of fatigue cracks, /9/.

TOTAL HIP REPLACEMENT IMPLANT

Selected implant 'Zimmer VerSys® CRC' is a modular stem, designed for fixation with bone cement (Fig. 1). The femur bone is in contact with the implant up to the bottom surface of the collar. Collar can be used for adding blocks if the surgeon has to compensate bone deficiencies. Two openings on the collar (Fig. 2-left) allow the block setting to implant using bolts, /10/. Other than these, the implant has one larger opening, 5 mm in diameter, and two smaller, both 3 mm in diameter (Fig. 2-right). The function of the smaller openings is to hold structures for fixation with the femur bone, which is optional, /10/. Larger opening and hole (Fig. 2-left) are intersected, and are assumed to have substantial influence on the stress distribution in the neck area of the implant.

The implant material must have superior mechanical properties, high yield and tensile strength and, in particular, high fatigue strength, /1/. The specified hip replacement 'Zimmer VerSys® CRC' is made of hot isostatic pressed F75 CoCrMo alloy (HIP Zimaloy), /11/. By a powder metallurgical process, a fine powder of cast alloy is compacted and sintered together under 100 MPa pressure and 1100°C for 1 hour. Then the alloy is forged to final shape. This process largely improves microstructural and mechanical properties of the alloy (Table 1), /11/. Based on the values in Table 1, the HIP Zimaloy delivers significant improvement especially in the case of fatigue strength.

Table 1. Mechanical properties of HIP Zimaloy, /10/.

	Yield stress (MPa)	Tensile strength (MPa)	Young's modulus (MPa)	Fatigue strength (MPa)
HIP Zimaloy	841	1277	253000	725-950
F75 CoCrMo	448-517	655-889	210000	207-310

FINITE ELEMENT METHOD

The stress distribution in the specified implant is computed using a commercial code for finite element method-Abaqus/CAE. A numerical 3D model of the specified implant is previously created. The 3D model is developed using SolidWorks software (Fig. 3-left). A simplification of the 3D model is required for numerical analysis to remove details not relevant for simulation (Fig. 3-left, red circle details). Roundings are excluded, except one between neck and stem (Fig. 3-left, marked green). Designated rounding has an undoubted influence on the stress distribution in the neck area of implant, because it stands in between the neck and openings with a hole. The bottom portion of stem and both openings on the collar are also excluded. A created simplified model is shown in Fig. 3-right.

Four simplified 3D models with different set of openings and hole are created for numerical analysis (Fig. 4):

- model 1: complete model with all openings and hole,
- model 2: with 5 mm opening and hole,
- model 3: with 5 mm opening,
- model 4: without any opening and hole.

Obtained 3D models are then converted to numerical models using Abaqus/CAE software (Fig. 5).

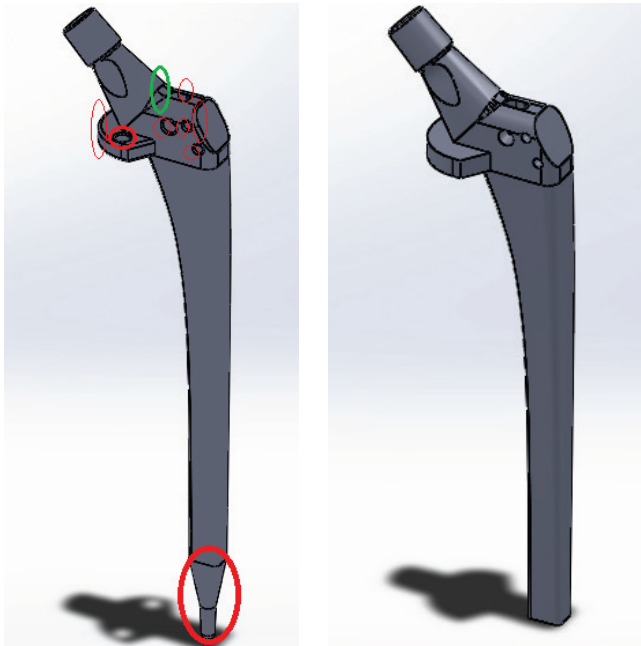


Figure 3. 3D model of implant: (left) complete 3D model; (right) simplified 3D model.

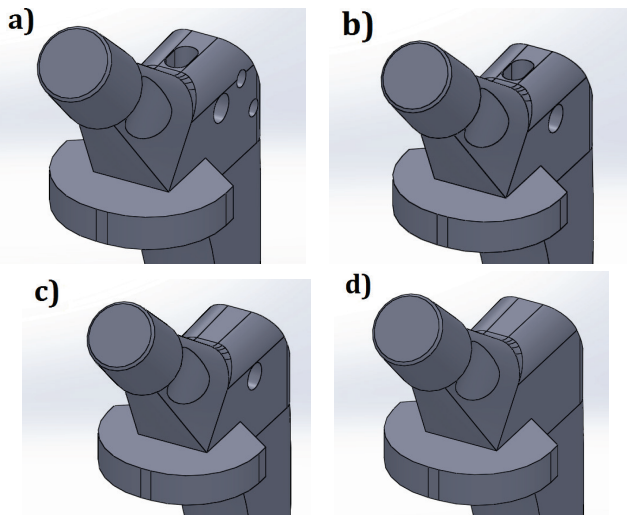


Figure 4. Four 3D implant models: (models 1-4).

The boundary condition is defined as fixed on surfaces that go into the medullary canal. The bottom of the collar lies on the bone, constrained in the vertical direction (Fig. 6).

Total hip replacement implants are exposed to periodic alternating loads which occur due to the cycle of walking. Physical activities transmit significant body weight to the hip joint. Unexpected events such as stumbling can generate resultant forces on the hip joint as much as 8.7 times body weight, which is an example of the highest measured resultant force on the hip joint, /4/. In this paper numerical analysis is performed for a maximal measured load on a patient of 90 kg mass. The resultant force to which the implant is then subjected is equal to 7681.23 N. It acts over the ball head and transmits load on the top surface of the neck taper. Load is defined as pressure applied on the top surface of the neck taper. The diameter of the top surface of the taper is 11.6 mm, which makes this pressure equal to 72.68 MPa (Fig. 6-left).

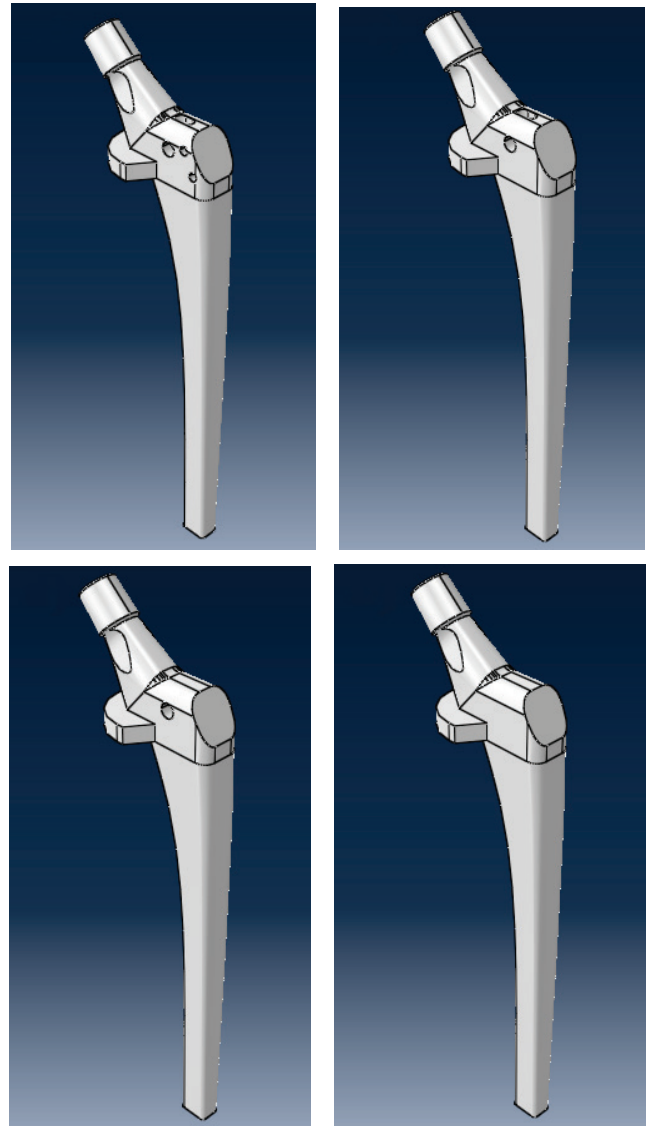


Figure 5. Corresponding numerical models.

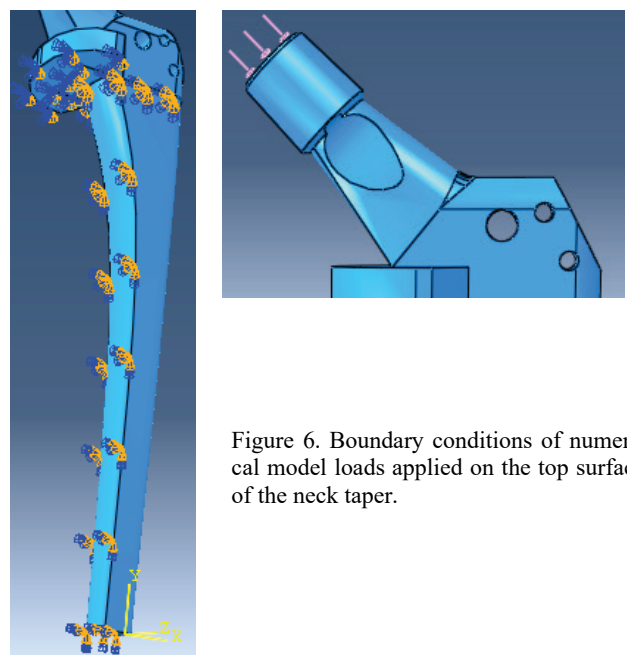


Figure 6. Boundary conditions of numerical model loads applied on the top surface of the neck taper.

Maximal applied stress on implant is well beneath yield stress of material (841 MPa), and in this static analysis the material is set as linear elastic with isotropic properties. Value of Young's modulus of selected material is given in Table 1 ($E = 253\,000\text{ MPa}$). Poisson's ratio is set as $\nu = 0.3$.

The mesh consists of a combination of tetrahedrons and hexahedrons. Parts with simpler shapes (i.e. collar, neck taper and supporting part that lies in a medullar canal) are filled with hexahedrons, and the rest is meshed with tetrahedrons (Fig. 7). Analysis is done with adopted global size of finite elements for the entire structure (global size-2).

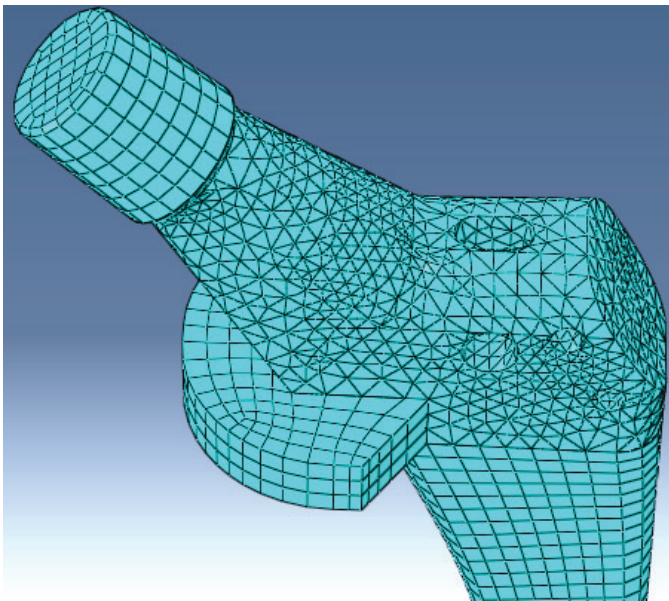


Figure 7. The FE mesh.

Number of acquired nodes, elements (tetrahedrons and hexahedrons) and values of maximal equivalent stresses, in each numerical model, are given in Table 2. Stress states are calculated according to the von Mises yield criterion.

Table 2. Number of nodes, elements and values of maximal von Mises stress in each model.

Numerical model	1	2	3	4
Nodes	34957	31566	29658	28235
Elements	24919	22892	21611	20479
Hexahedrons	8680	9060	9060	8452
Tetrahedrons	16239	13832	12551	12027
Max.stress (MPa)	125.7	125.2	122.9	118.7

According to Table 2, the number of hexahedrons is almost identical in all numerical models. This is because all parts meshed with hexahedrons are the same for every model. Absence of the exact equality is due to an error of automatic generation of elements and nodes in software. Models with more openings and a hole on the stem require more elements and nodes for meshing. The difference emerges from a number of tetrahedrons, which are applied for meshing areas around the openings and the hole. The maximal von Mises stress is located in the neck area of the implant, on sharp edges in all four numerical models - as expected (Figs. 8 and 9). They have approximate values, thus proving that an approximation of the model is adequate.

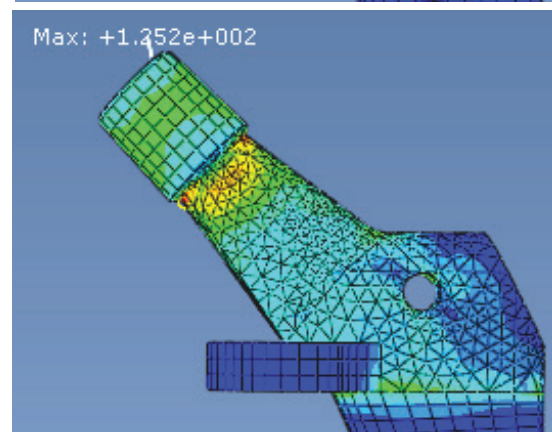
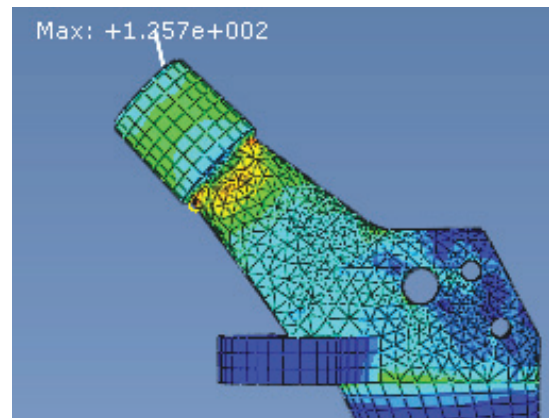


Figure 8. Von Mises stress distribution with marked maximal stress on: (top)-model 1; (bottom)-model 2.

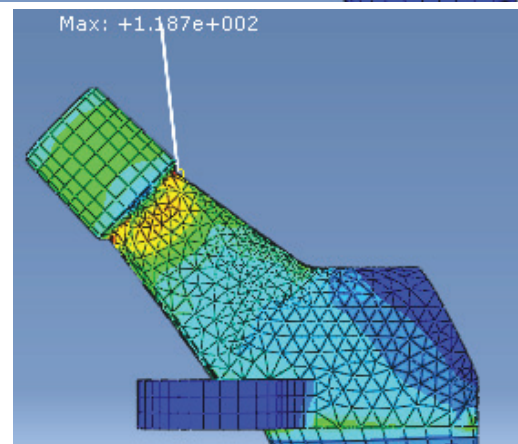
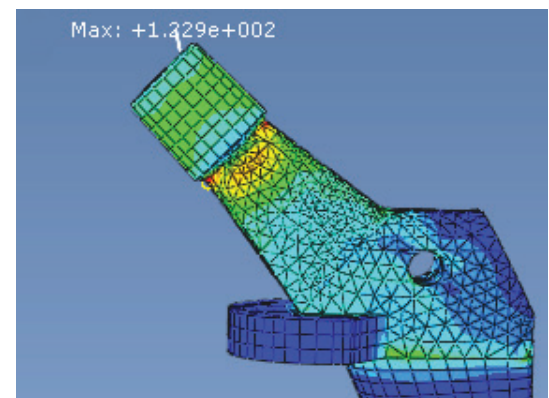


Figure 9. Von Mises stress distribution with marked maximal stress on: (top)-model 3; (bottom)-model 4.

RESULTS AND DISCUSSION

Calculated von Mises stresses in case of maximal static load in all four models are much smaller than the yield stress of the material ($Y_S = 841 \text{ MPa}$ - Table 1). Implant made of this material will not break under any static load.

Figures 8-top and 9-bottom show how all the openings and the hole on the stem influence the stress distribution of the neck area in the implant. Without openings and the hole (Fig. 9-bottom) maximal von Mises stress would appear on the tension side of the neck. In that area tensile stresses would tend to open the crack, which would lead to certain failure of the structure. Applied openings and hole on stem make stress distribution on complete neck area more even. The addition of all openings and hole to the structure shifts maximal stress concentration to the compressive zone, forcing the material to press an eventual crack, preventing its further propagation.

Stress states of both models 1 and 2 are approximate, with only 0.5 MPa difference between two maximal von Mises stresses (Fig. 8). This demonstrates that two smaller openings do not have a significant role in the stress distribution in the neck area of the implant.

At the intersection of the larger opening and the hole there are stress concentrations on sharp edges - symmetrical at both sides, with values up to 104.8 MPa (Fig. 10). These stress concentrations influence the stress distribution in the neck area of the implant. A larger opening coupled with a hole has a critical role in the stress distribution of the neck area of the selected total hip replacement implant. Individual roles of the larger opening and hole are explained through stress distribution in the neck area of numerical models 2, 3 and 4 (Figs. 11, 12 and 13).

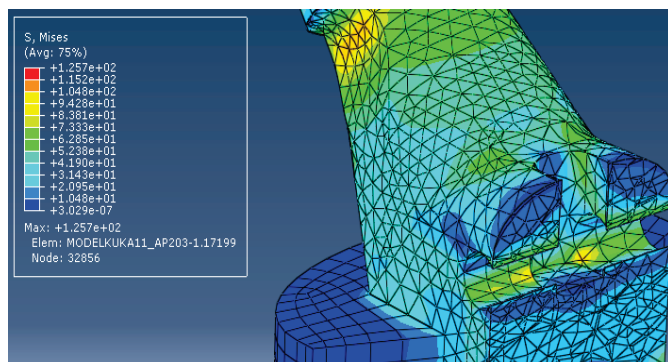


Figure 10. Stress state at intersection of larger opening and hole.

Stress distribution in the neck area of model 3 (Fig. 12) shows that a larger opening shifts maximal von Mises stress to the compression side of the implant neck, thus reducing stresses in the tension zone (compared with model 2 - Fig. 11). But then in the compression zone there is a larger stress concentration area along the sharp edge (Fig. 12-top).

Adding a hole to the structure (model 2) increases the maximal stress in the compression zone, from 122.9 MPa to 125.2 MPa, but reduces a stress concentration area in the compression zone (Fig. 13-top). Figure 13-bottom shows that a further reduction of stresses in the tension zone occurs. The analysed implant is designed to press the eventual crack, which largely increases structural life.

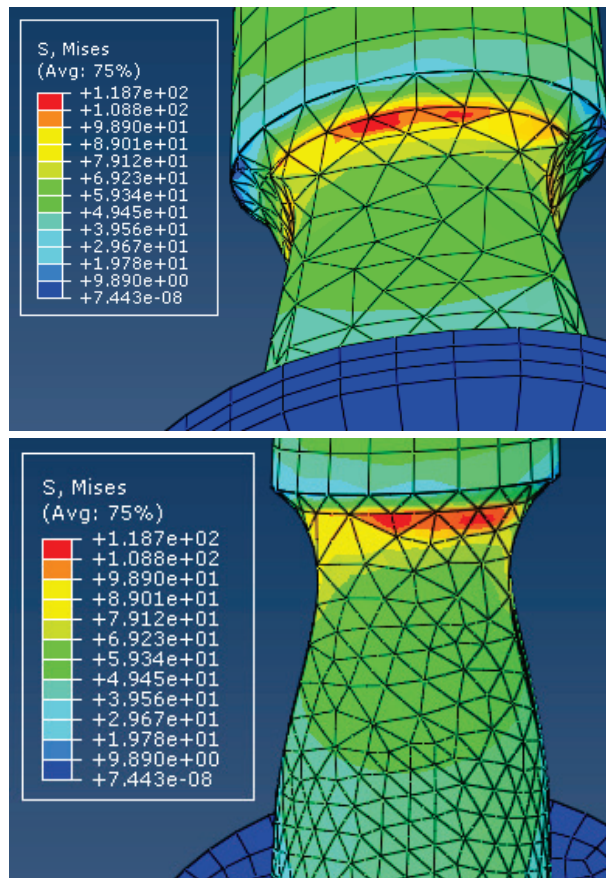


Figure 11. Von Mises stress distribution of model 4: (top) at bottom of the neck; (bottom) at top of the neck.

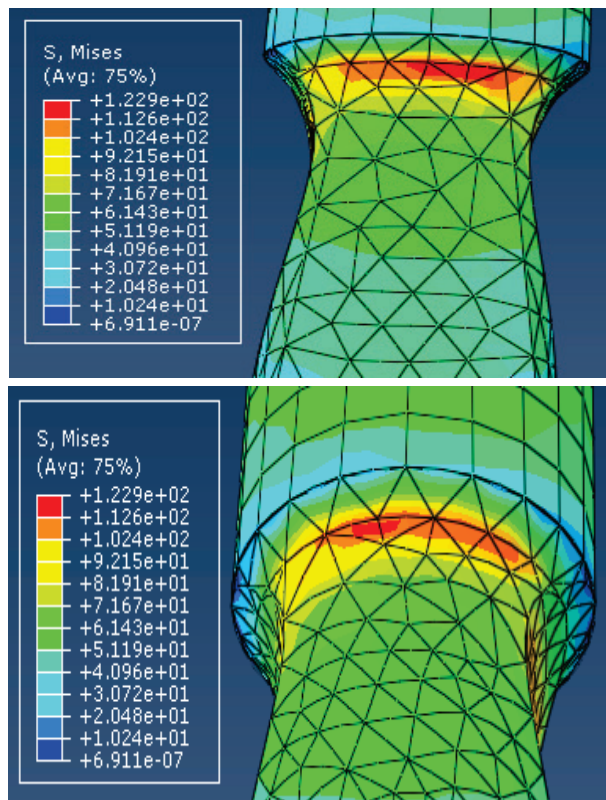


Figure 12. Von Mises stress distribution of model 3: (top) at bottom of the neck; (bottom) at top of the neck.

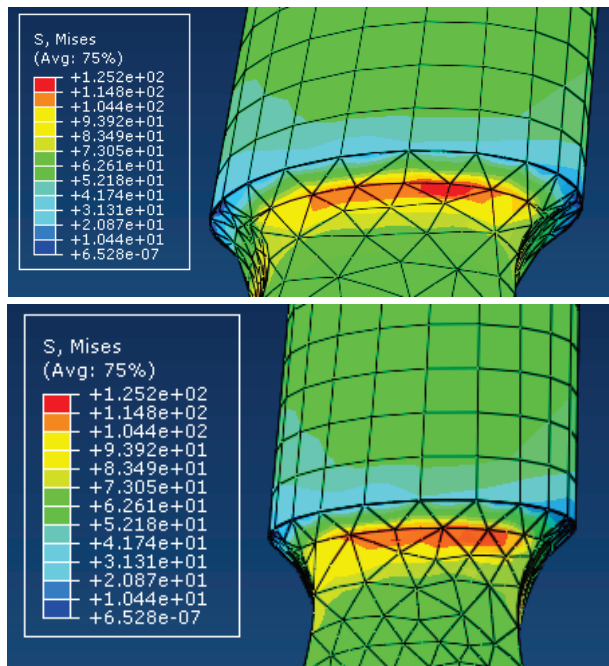


Figure 13. Von Mises stress distribution in model 2: (top) at bottom of the neck; (bottom) at top of the neck.

It should be noted that the accuracy of this numerical analysis depends on assumptions and approximations. The dimensions are obtained by manual measurement, which does not guarantee absolute accuracy. Simplifications of the 3D model are done to remove details not relevant for simulation. Defining the material with only two parameters for a large number of cases is enough, but could lead to inaccurate results. Boundary conditions are based on the assumptions of the behaviour of bone-implant contact. Concerning the load direction, it is assumed to act perpendicularly to the top surface of the neck taper. It is worth mentioning that the human body is a highly corrosive environment, which greatly affects creation and widening of fatigue cracks, whose influence we have not considered. To obtain the best results, it is necessary to introduce as few as possible assumptions and approximations.

CONCLUSIONS

The neck area of the total hip replacement implant represents a critical area for crack initiation. In four numerical models it has been shown how certain design solutions influence the stress distribution in the neck area of the particular total hip replacement implant. The individual influence of applied openings and the hole is analysed in order to show how they affect the eventual crack behaviour.

Total hip replacement implants are designed to enable actual hip movement. In many cases implant designs have to balance between movement ability and structural life. Better use of the implant and patient commodity often is at the expense of higher stress distribution in the structure.

Numerical analysis provides satisfactory results in predicting mechanical behaviour of the total hip replacement implants. In spite of great mechanical properties of materials used in orthopaedics, total hip replacement implants are designed to prevent eventual crack propagation. Implant

designs with maximal stress concentration in areas that are under compression stresses would preclude eventual crack propagation, increasing implant structural life.

REFERENCES

1. Milne, I., Ritchie, R.O., Karihaloo, B., *Comprehensive Structural Integrity, Vol.9: Bioengineering*. Amsterdam, London, Elsevier Ltd., 2003.
2. Sedmak, A., Čolić, K., Burzić, Z., Tadić, S. (2010), *Structural integrity assessment of hip implant made of cobalt-chromium multiphase alloy*, *Struct. Integ. & Life*, 10(2):161-164.
3. Maehara, K., Doi, K., Matsushita, T., Sasaki, Y. (2002), *Application of vanadium-free titanium alloys to artificial hip joints*, *Mater. Trans.*, 43(12):2936-2942.
4. Byrne, D., Mulhall, K., Baker, J. (2010), *Anatomy & biomechanics of the hip*, *The Open Sports Med. J.*, 4:51-57.
5. Hughes, P., Hsu, J., Matava, M. (2002), *Hip anatomy and biomechanics in the athlete*, *Sports Med. & Arthrosc. Rev.*, 10(2):103-114.
6. Čolić, K., Sedmak, A., Grbović, A., et al. (2016), *Numerical simulation of fatigue crack growth in hip implants*, *Procedia Engng.*, 149: 229-235.
7. Čolić, K., Sedmak, A., Grbović, A., et al. (2016), *Finite element modelling of hip implant static loading*, *Procedia Engng.*, 149: 257-262.
8. El-Sheikh, H. El-Din, Mac Donald, B.J., Hashmi, M.S.J. (2003), *Finite element simulation of the hip joint during stumbling: a comparison between static and dynamic loading*, *J Mat. Proc. Techn.*, 143-144: 249-255.
9. Edwards, B.J., Louthan, M.R.Jr, Sisson, R.D.Jr, *Hydrogen embrittlement of zimaloy: a cobalt-chromium-molybdenum orthopedic implant alloy*, 2nd Int. Symp. on Corrosion and Degrad. of Implant Mat., Eds. A. Fraker, C. Griffin, ASTM STP 859, 1985, pp.11-29.
10. Zimmer Inc. (2007), *Zimmer VerSys® CRC-Cemented Revision/Calcar Hip System* [brochure].
11. Ratner, B., Hoffman, A., Schoen, F., Lemons, J., *Biomaterials Science - An Introduction to Materials in Medicine*, Academic Press, 1996.

© 2017 The Author. Structural Integrity and Life, Published by DIVK (The Society for Structural Integrity and Life 'Prof. Dr Stojan Sedmak') (<http://divk.inovacionicentar.rs/ivk/home.html>). This is an open access article distributed under the terms and conditions of the [Creative Commons Attribution-NonCommercial-NoDerivatives 4.0 International License](#)